

PCCP

Accepted Manuscript



This is an *Accepted Manuscript*, which has been through the Royal Society of Chemistry peer review process and has been accepted for publication.

Accepted Manuscripts are published online shortly after acceptance, before technical editing, formatting and proof reading. Using this free service, authors can make their results available to the community, in citable form, before we publish the edited article. We will replace this *Accepted Manuscript* with the edited and formatted *Advance Article* as soon as it is available.

You can find more information about *Accepted Manuscripts* in the [Information for Authors](#).

Please note that technical editing may introduce minor changes to the text and/or graphics, which may alter content. The journal's standard [Terms & Conditions](#) and the [Ethical guidelines](#) still apply. In no event shall the Royal Society of Chemistry be held responsible for any errors or omissions in this *Accepted Manuscript* or any consequences arising from the use of any information it contains.

Hydrogen-atom attack on phenol and toluene is ortho-directed.

Olha Krechkivska,^a Callan M. Wilcox,^a Tyler Troy,^{b,§} Klaas Nauta,^a Bun Chan,^b Rebecca Jacob,^b Scott A. Reid,^c Leo Radom,^b Timothy W. Schmidt,^a and Scott H. Kable^a

a) School of Chemistry, University of New South Wales, Kensington, NSW, 2052, Australia

b) School of Chemistry, University of Sydney, Sydney, NSW, 2006, Australia

c) Department of Chemistry, Marquette University, Milwaukee, WI, 53201, USA.

† *Electronic supplementary information (ESI) available: Experimental measurement of excited lifetime and the complete set of theoretical data.*

§ *Present address: Chemical Sciences Division, Lawrence Berkeley National Laboratory, MS 6R-2100, Berkeley, CA, USA*

Abstract:

The reaction of H + phenol and H/D + toluene has been studied in a supersonic expansion after electric discharge. The (1+1')-resonance-enhanced multiphoton ionization (REMPI) spectra of the reaction products, at $m/z = \text{parent} + 1$, or $\text{parent} + 2$ amu, were measured by scanning the first (resonance) laser. The resulting spectra are highly structured. Ionization energies were measured by scanning the second (ionization) laser, while the first laser was tuned to a specific transition. Theoretical calculations, benchmarked to the well-studied H + benzene \rightarrow cyclohexadienyl radical reaction, were performed. The spectrum arising from the reaction of H + phenol is attributed solely to the *ortho*-hydroxy-cyclohexadienyl radical, which was found in two conformers (*syn* and *anti*). Similarly, the reaction of H/D + toluene formed solely the *ortho* isomer. The preference for the *ortho* isomer at 100-200 K in the molecular beam is attributed to kinetic, not thermodynamic effects, caused by an entrance channel barrier that is ~ 5 kJ mol⁻¹ lower for *ortho* than for other isomers. Based on these results, we predict that the reaction of H + phenol and H + toluene should still favour the *ortho* isomer under elevated temperature conditions in the early stages of combustion (200 – 400°C).

Introduction

Addition, loss, and transfer of hydrogen atoms constitute some of the most fundamental processes in chemistry. Loss of a hydrogen atom is the first chemical step in most combustion processes.¹ OH radical abstraction of H starts the atmospheric oxidative process for many airborne organic compounds, and further abstraction of H from free radicals by O₂ continues the pathway.² Intramolecular H-atom transfer promotes isomerization between various isomers, for example, gas-phase keto-enol tautomerization.³ Hydrogenation and dehydrogenation of polycyclic aromatic hydrocarbons (PAHs) are also hypothesized to occur in the interstellar medium.⁴⁻⁶ Indeed, throughout chemistry, the energetic and kinetic battle between molecules, radicals and ions in competition for H atoms is prevalent throughout all complex reaction mechanisms.

Aromatic molecules constitute a large fraction of many liquid fuels, including automotive petroleum/gasoline. The Australian standard allows automotive fuel to comprise up to 45% aromatics by weight.⁷ The addition of H₂ to such aromatic fuel mixtures has long been known to result in a much lower production of soot, which is largely comprised of PAHs.⁸ The effectiveness of H₂ in reducing soot formation has been attributed to sequential addition of H atoms to the aromatic core, until the ring is entirely saturated. For example, benzene is converted to cyclohexane, toluene to methylcyclohexane.⁹

Despite extensive modelling of H-addition to aromatic compounds, the intermediate H-adducted radicals have rarely been detected. The cyclohexadienyl radical itself (H+benzene) is well characterized.¹⁰⁻¹³ Additionally, several reports characterizing the hydronaphthyl radical (H+naphthalene) have been reported recently.¹⁴⁻¹⁸ However, the spectroscopy, structure, energetics and kinetics of H-addition to other common aromatics, such as toluene and phenol, are largely unreported.

In this paper, we report the spectroscopic characterization of the radicals formed from H-addition to two singly-substituted aromatic molecules – phenol and toluene. Toluene and phenol are prototypical functionalized benzene compounds that also find general application. Toluene is a common fuel additive. H-atom attack leads to one of four isomeric methyl-cyclohexadienyl (methyl-CHD) radicals (Fig 1), and is an important combustion reaction. H-addition to phenol leads to the hydroxy-cyclohexadienyl

(hydroxy-CHD) radical. The *ipso* isomer of this radical (Fig 1) is the same species that is formed from OH attack on benzene, which is the postulated first reaction in the oxidation of aromatic species in the atmosphere.¹⁹

Previous work on CHD, hydroxy-CHD and methyl-CHD

The $D_1 - D_0$ energies and ionization energies (IEs) of hydroxy- and methyl-CHD are key experimental observables in the present work. Comparison with the results of quantum chemistry computations allows us to decide which isomers are observed.

Cyclohexadienyl radical is used to benchmark our theoretical methods because both the $D_1 - D_0$ transition¹⁰⁻¹² and IE are well-known,¹³ and there have been two recent computational studies with which to compare our methods.^{13,20}

The electronic absorption spectrum of the CHD radical was first reported in 1963 in a frozen (77 K) matrix of 3-methylpentane, revealing two maxima near 310 nm.²¹ Several measurements have been made subsequently,^{22,23} concluding that this transition corresponds to excitation of the second excited electronic state. The $D_1(2A_2) - D_0(2B_1)$ electronic band system of CHD was found to lie in the visible region of the spectrum, near 550 nm.¹⁰ High-resolution laser-induced fluorescence (LIF) spectra in the gas phase identified the electronic origin at 18,207 cm⁻¹.¹⁰⁻¹² The IE of CHD has been reported recently to be 6.820(1) eV.¹³

Experimental²⁴⁻²⁶ and theoretical²⁷⁻³⁰ investigations of hydroxy-CHD have mostly approached this species from the benzene + OH side because of the atmospheric relevance. A consequence, however, is that the *ipso* form of the radical has been almost solely considered; the *ortho*, *meta* and *para* forms have received much less attention. Hydroxy-CHD has been detected in the gas phase by UV absorption spectroscopy via the $D_2 - D_0$ transition, near 300 nm.^{26,30} The UV spectrum is broad, like CHD.³⁰ Neither the $D_1 - D_0$ spectrum, nor the IE, has been reported for any isomer.

The methyl-CHD radical has received relatively little attention. Uc *et al.* have calculated the relative stability, $\Delta H_f(298\text{ K})$, of all four methyl-CHD isomers relative to toluene + H.³¹ Tokmakov and Lin calculated the reaction profile for H + toluene \rightarrow *ipso*-methyl-

*H-addition to phenol and toluene**submitted to PCCP*

CHD and thence to benzene + CH₃.³² They also calculated the barrier to the [1,2]-H shift between *ipso* and *ortho* isomers to be vastly in excess of the C-H bond energy. To our knowledge, the electronic spectroscopy of methyl-CHD, including the IE has not been reported.

Experimental and Computational Methods

Experimental

Experiments were carried out in a resonance-enhanced multiphoton ionization (REMPI) chamber equipped with a time-of-flight (ToF) mass spectrometer that has been described previously.³³ The vapor of phenol or toluene (Aldrich, used as supplied) was co-expanded with H₂O/D₂O in a free jet expansion using Ar carrier gas at a seed ratio of ~0.1-1% organic, ~1% water at a total pressure of 6-7 bar. The gas mixture entered the vacuum via a pulsed nozzle equipped with a pair of electrodes. During the gas pulse, a short (80 μs) high-voltage pulse (1.6 kV with 25 kΩ ballast resistor) sparked an electric discharge. During the discharge, metastable Ar atoms collide with H₂O / D₂O molecules, fragmenting them to H + OH (D + OD) with high efficiency.³⁴ H/D atoms in turn collide with the aromatic species. In the high-pressure region of the expansion, there are sufficient three-body collisions to stabilize the H-adducted radicals.

The expansion is passed through a skimmer ($\phi = 2$ mm) forming a collimated molecular beam in the ionization chamber. The beam was intersected with two tunable ns-pulsed laser beams, counter-propagating and coincident in time. The first beam (Nd:YAG-pumped dye laser) excited the $D_1 - D_0$ transition in the H-adducted radical, which was near 550 nm in each case (C540A dye). A second Nd:YAG-pumped dye laser, tuned near 300 nm (R610 dye and a BBO doubling crystal), served to ionize the excited radical.

The closed-shell cation formed after REMPI was accelerated in a ToF mass spectrometer and detected via a multichannel plate detector. The signal on the m/z (parent+1 or parent+2) mass was monitored as a function of either laser wavelength or delay time between lasers. Scanning the first laser, with the second laser well above the ionization threshold, provided a REMPI spectrum of the $D_1 - D_0$ transition of the radical. Scanning

the second (ionization) laser while holding the first laser on a resonance provided a photoionization efficiency (PIE) spectrum and hence the ionization energy.

Hole-burning experiments were performed to distinguish different isomers. In these experiments, the two lasers used above were tuned to a peak in the REMPI spectrum. A third laser (Nd:YAG-pumped dye laser) intersected the molecular beam about 100 ns before the REMPI lasers. This laser was scanned across the same wavelength range as the $D_1 - D_0$ spectrum and was used to “bleach” the population of whichever radical was in resonance with that laser. If the isomer was the same as being probed by REMPI, then the bleach results in a smaller REMPI signal. If the bleach laser depletes a different isomer, then the REMPI signal is unaffected. In this way, an isomer-specific hole-burning spectrum (depletion of REMPI signal) is measured as a function of bleach wavelength.

Theoretical

Standard *ab initio* and density functional theory (DFT) calculations were carried out using the Gaussian 09³⁵ and MOLPRO 2010³⁶ programs. Lower-level calculations were carried out using the (TD)-B3-LYP DFT procedure and appropriate basis sets. Higher-level calculations were carried out with composite methods that aim to approximate CCSD(T) with an infinite basis set, either by additivity and empirical corrections, or via extrapolation. The former category includes G3X(MP2)-RAD³⁷ and G4(MP2)-6X,³⁸ while the latter includes W1X-1³⁹ and W1X-2,³⁹ with W1X-1 being slightly more accurate.³⁹ Geometries for the G3X(MP2)-RAD calculations were optimized at the B3-LYP/6-31G(2df,p) level. The resulting single-point energies were corrected (where indicated) with zero-point energies (zpe’s) and thermal corrections, derived from scaled (0.9854) B3-LYP/6-31G(2df,p) harmonic vibrational frequencies, to provide enthalpies at 0 K and 298 K. For the G4(MP2)-6X procedure, geometries were optimized at the BMK/6-31+G(2df,p) level,⁴⁰ and the energies corrected to enthalpies at 0 K and 298 K using zpe and thermal corrections, derived from scaled (0.9770 and 0.9627, respectively) BMK/6-31+G(2df,p) harmonic vibrational frequencies.⁴¹ The geometries for W1X-1 and W1X-2 were obtained using B3-LYP/cc-pVTZ+d. Scaled (by 0.985) B3-LYP/cc-pVTZ+d harmonic vibrational frequencies were used to obtain zpe’s and thermal corrections, which were incorporated as required to give enthalpies at 0 K and 298 K.³⁹

Results

Theoretical Benchmarking Study

Computational chemistry is an important ingredient in the assignment of the carriers of the m/z 95 (H + phenol) and m/z 93 (H + toluene) spectra. Therefore we performed a series of benchmarking calculations on the cyclohexadienyl (CHD) radical.

Several groups have calculated ionization and bond energies of the CHD radical.^{20,42,43} The most recent, and highest level calculations, were performed by Botschwina and co-workers, who reported various ionization and bond-breaking properties of CHD using explicitly correlated coupled cluster theory at the (R)CCSD(T)-F12 level.²⁰ The calculated ionization energy was 6.803(5) eV, which compares very favorably with the new experimental result, 6.8201(5) eV,¹³ although the computational error seems to be slightly underestimated. We use these computational results and a variety of experimental results for benchmarking our computational methods.

Table 1 shows calculated values of the IE of CHD, the proton affinity of benzene, and the strength of the C-H bond in both C_6H_7 and $C_6H_7^+$, for several theoretical procedures and basis sets. DFT is computationally efficient, and has been shown to produce good nuclear geometries and vibrational frequencies.²⁰ However, it performs less well in reproducing ionization and bond-breaking energies with an IE that is 300 meV lower than the previous (R)CCSD(T*) calculation and a proton affinity that is 60 kJ mol⁻¹ too high, compared with experiment (Table 1).⁴⁴⁻⁴⁶

Higher-level electronic structure calculations were performed at the optimized B3-LYP/6-31G(2df) geometry. The three *ab initio* methods, G3X(MP2)-RAD, G4(MP2)-6X and W1X-1, and to a lesser extent, B3-LYP with a larger basis set, all perform much better and we benchmark them against (R)CCSD(T*)²⁰ and experiment.¹³ For neutral C_6H_7 , the vibrationless (pure electronic) energies are all within 100 meV for the IE, and within 3 kJ mol⁻¹ for the C-H bond energy of the previous (R)CCSD(T*) results.²⁰ When corrected for zpe, the IE calculated using W1X-1 is very close to the experimental measurement. Indeed the W1X-1 and (R)CCSD(T*) calculations bracket the experimental IE, with the deviations in each case being only 20 meV. When a thermal

correction is applied to the 0 K values, the W1X-1 bond energy and proton affinity at 298 K are within 4 kJ mol⁻¹ of the experimental (298 K) values.

G3X(MP2)-RAD and G4(MP2)-6X theory are slightly less accurate than W1X-1 and (R)CCSD(T) for the four experimental observables in Table 1, but are computationally more efficient. Specifically, the zpe-corrected ionization energy is over-estimated by 80 meV and we use this as an empirical correction factor for G4 theory in estimating IEs for the larger radicals below.

H-addition to phenol: hydroxy-cyclohexadienyl radical (hydroxy-CHD)

Figure 2a shows the (1+1') REMPI spectrum of the species at m/z 95 from a discharge of phenol and water in argon that has been expanded in a molecular beam. The two strongest peaks, near 18,200 cm⁻¹, are separated by only 18 cm⁻¹, in the region that we associate with the $D_1 \leftarrow D_0$ electronic origin transition.

Photoionization efficiency (PIE) curves were recorded following excitation of these two strongest peaks, as shown in Fig 3. The IEs shown in the figure were recorded with an extraction field of 206 V, which lowers the true IE slightly. We have previously measured the effect of the electric field on the IE of methyl-CHD and found that the extrapolated zero-field IE was 8±1 meV higher than measured under these operating conditions.¹³ While different molecules will be affected differently by an external field, the orbitals from which the electron is ejected in methyl-CHD and hydroxy-CHD are similar. Therefore the correction from observed to zero-field IE should also be very similar for both molecules, and we have used the same correction factor for both. These corrected values are shown in Table 2. The ionization thresholds for the two isomers are very close, differing by only 10.2 meV (82 cm⁻¹). However, this is considerably in excess of our experimental uncertainty, which we estimate at <1 meV (8 cm⁻¹), which reinforces the finding that there are two isomers present in the spectrum.

Two hole-burning spectra were measured, shown reflected below the REMPI spectrum in Fig 2. In this experiment, the REMPI lasers were tuned to the frequency of one of the major peaks at 18,200 (spectrum b) or 18,218 cm⁻¹ (spectrum c). The bleach laser, 100 ns earlier in time, was scanned through the same region. The hole-burning spectra show

*H-addition to phenol and toluene**submitted to PCCP*

clearly that the two major peaks near 18,200 cm⁻¹ belong to different isomers. Additionally, the two hole-burning spectra identify every major peak in the spectrum with one or the other isomer. Therefore we conclude that the REMPI spectrum in the region shown in Fig 2a comprises only 2 isomers.

Finally, the ionization laser was scanned in time across the laser responsible for $D_1 \leftarrow D_0$ excitation. This temporal scan, shown in Supplementary Information, was fit to a convolution of an 8 ns Gaussian function (the instrument function) and a decaying exponential function to provide an estimated lifetime of the D_1 state of 4 ± 1 ns.

There are four structural isomers of the hydroxy-CHD radical, formed from H-addition to the benzene ring in the *ortho*, *meta*, *para* and *ipso* positions with respect to the hydroxyl group (Fig 1). We turn to theory to distinguish which of the four isomers are the carriers of the observed spectrum.

Table 2 shows selected computational results for the four isomers of hydroxy-CHD at the G4(MP2)-6X level of theory. The most directly comparable quantity for distinguishing between the isomers is the IE. Based on the benchmark studies against CHD, we expect the calculated G4(MP2)-6X value to over-estimate the experimental IE by about 80 meV. Table 2 shows the predicted IEs, using our empirical correction factor for all four isomers. Experimentally, two IEs were measured: 6.399(1) and 6.409(1) eV. Only one computational IE lies near these values – the corrected IE of *ortho*-hydroxy-CHD was calculated to be 6.39 eV. The IE's of all other isomers lie >0.25 V higher or lower than the experimental values and therefore we conclude that *para*, *meta* and *ipso*-hydroxy-CHD are *not* the carriers of the spectrum.

A potential energy scan of the OH torsional angle, with other coordinates optimized at each OH angle, is shown in Fig 4, showing that there are two conformers of the *ortho*-hydroxy-CHD radical. The *anti* isomer lies about 450 cm⁻¹ to lower energy than *syn*, with a 1750 cm⁻¹ barrier (measured from the *anti* side) between them. The relative energies are sufficiently similar and the interconversion barrier sufficiently high, that both rotamers are likely to be formed in the expansion.

To further explore the REMPI spectra, we performed TD-DFT (B3LYP/cc-pvtz) calculations on the D_1 excited states of both *syn* and *anti*-*ortho*-hydroxy-CHD radical.

Table 3 shows the calculated vertical transition energy, zero-point energy (zpe) corrected energy and oscillator strength for these species with the same calculations for the CHD radical shown for comparison. In CHD, the experimental $D_1 - D_0$ transition energy is 2230 cm^{-1} lower than the calculation;^{11,12} the $D_1 - D_0$ transition energies of both *syn* and *anti* isomers of ortho-hydroxy-CHD are over-estimated by a similar amount. The transition in the *anti* isomer is predicted to be of lower energy than the *syn*, although the computational difference is greater than the experimental difference. The oscillator strength is calculated to be about twice as strong for the *anti* conformer compared with the *syn*. Consideration of the experimental ionization energies, the transition energies and intensities, compared with theory, leads us to assign the more intense transition at $18,200 \text{ cm}^{-1}$ to the lower energy, *anti* isomer and the weaker transition, displaced 18 cm^{-1} to higher energy, to the *syn* isomer.

Using the D_1 harmonic vibrational frequencies from these calculations, we have been to completely assign the spectra of both *syn* and *anti* conformers. A complete discussion of this spectroscopic assignment, including the role of in-plane and out-of-plane vibrations, change of OH torsional angle, Fermi resonance and the strengths and weaknesses of the calculations is beyond the scope of this paper. Such detailed spectroscopic analysis does not add to the purpose of this paper, which is a description of *ortho* directing nature of the H + phenol reaction. Here, we summarise the key spectroscopic results:

- i) every transition in the REMPI spectrum can be assigned to transitions of the *syn* and *anti* conformers of ortho-hydroxy-CHD. No line with any appreciable intensity remains unassigned;
- ii) the assignments can only be made with the *anti* isomer assigned as the lower frequency, more intense transition, as hypothesized above;
- iii) the most intense transitions for each conformer are loosely associated with the ring-breathing vibration in benzene,⁴⁷ shifted to lower frequency as is common in singly- and di-substituted benzene compounds;^{48, 49}
- iv) The calculated minimum energy structure in the D_1 state shows a non-planar distortion of the ring. Assignment of both *syn* and *anti* spectra required activity in out-of-plane vibrations. This is consistent with the calculated non-planar structure in the D_1 state;

- v) the *syn* conformer also shows significant intensity in the vibrational modes loosely affiliated with the ν_6 and ν_{18} modes in benzene,⁵⁰ again consistent with similar activity in these modes in activity in singly- and di-substituted benzenes.^{48,49}
- vi) calculations show that in-plane and out-of-plane vibrations are significantly more mixed for vibrations of the *anti* conformer in the D_1 state. There is no analogous vibration for mode 6a in benzene (in-plane ring deformation) for this molecule; the activity is spread through close-lying levels. This is reflected by several transitions calculated and observed in the vicinity of the 6a vibrational frequency (Fig 2). The benzene labels are no longer a good description of the modes in the *anti* conformer. This effect has been discussed in detail previously for other substituted benzenes.⁵¹

We have indicated a few of the key assignments above the spectrum in Fig 2. A full description of the spectroscopy of these species, along with the methyl-CHD species, will be published in a forthcoming full spectroscopy paper. Our conclusion for the present work is that the ionization potential, D_1 - D_0 frequency, and vibrational frequencies support the REMPI spectrum in Fig 2 being comprised *solely* the *syn* and *anti* conformations of the *ortho*-hydroxy-CHD radical.

Searching for other m/z 95 isomers: We have also performed TD-DFT (B3LYP/cc-pvtz) calculations on the D_1 excited states of the *ortho*, *meta* and *para* isomers of hydroxy-CHD, including *syn* and *anti* conformers of the *meta* isomer. Table 3 shows the calculated vertical transition energies and zero-point energy (zpe) corrected energies, T_{00} , for each isomer. While the vertical calculations for the *ipso* isomer in the D_1 state did converge, they would not optimize to the minimum of the D_1 state at this level of theory. The calculations appeared to find a conical intersection with the ground electronic state. It is not clear whether this conical intersection is real, or a vagary of the level of theory. Much higher levels of theory will be required to address this. Nonetheless, a vertical transition energy and oscillator strength were able to be calculated and are reported in Table 3.

If we assume that the computational error will be similar (i.e. $2000 \pm 200 \text{ cm}^{-1}$ too high) for the evaluated CHD and *ortho*-hydroxy-CHD and the, as yet, unobserved isomers, then the *meta* isomer should absorb in a similar region to that in Figure 2, while the *para* isomer is predicted to absorb considerably further to the red, near $15,000 \text{ cm}^{-1}$. For each radical (including CHD itself), the calculated vertical transition energy is $1,900 \pm 500 \text{ cm}^{-1}$ higher than the calculated T_{00} . If we assume the same to be true for the *ipso* isomer, then we predict this isomer will absorb at about $22,400 - 1900 - 2000 = 18,500 \text{ cm}^{-1}$, which also lies within the region shown in Figure 2.

To search for the other isomers, we performed a series of experiments with the ionization laser wavelength set to 230 nm, while the resonance ($D_1 \leftarrow D_0$) laser was scanned from 617 to 480 nm. This combination of wavelengths provides a total energy of 7.4 – 8.0 eV, which is in excess of the ionization energy of all isomers according to the calculations in Table 2. The range 617 to 480 nm ($16,200 - 20,800 \text{ cm}^{-1}$) is sufficient to encompass the range of $D_1 - D_0$ energies for all isomers, as shown in Table 3, even allowing for a likely $\sim 9\%$ over-estimate of the theory. The only additional structures found in this range were two small peaks near $17,714$ and $17,865 \text{ cm}^{-1}$, as shown in the inset to Fig 2. The intensity of these peaks is similar, and about $30\times$ weaker than the strong origin bands of *ortho*-hydroxy-CHD. The peaks were too weak to measure a PIE spectrum. The displacement of the two new peaks from the strong *ortho*-hydroxy-CHD transitions cannot be assigned readily to low frequency vibrations of ground-state *ortho*-hydroxy-CHD radical according to our calculations of the vibrational frequencies. Also, their intensity did not seem to scale with that of other hot bands (e.g. just to the red of the origin transitions). Therefore they do not seem to be hot bands of the *ortho*-hydroxy-CHD spectrum.

The two new transitions are about 500 cm^{-1} lower than the *ortho*-hydroxy-CHD origin and this difference is in accord with that calculated for the *meta* hydroxy-CHD radical relative to the *ortho* isomer. In addition, their larger splitting of 150 cm^{-1} is in accord with the larger calculated *syn* - *anti* splitting, and the similar intensity is consistent with the calculated oscillator strengths (Table 3). Therefore we tentatively assign these two peaks to the *syn* and *anti* rotamers of the *meta* species. If this assignment is correct, then the *meta* isomer is formed at $<1\%$ of the population of the *ortho*, given the $30\times$ weaker spectrum, and $10\times$ higher oscillator strength. However, we cannot conclusively rule out

hot bands, nor a different constitutional isomer of C_6H_7O and this assignment must be considered to be tentative.

The *ipso* isomer has a calculated $D_1 \leftarrow D_0$ transition energy that is similar to that of the *ortho* (Table 3). Hole burning shows that all major peaks in Fig 2 are attributable to the *ortho* isomers. However, the lower signal-to-noise ratio of the hole-burning spectra makes it difficult to conclude that the spectrum of the *ipso* isomer is not hiding in the weaker, more complex structure at the blue end of this spectrum. Therefore we used the fact that the calculated IEs for *ortho* and *ipso* isomers are quite different and re-measured the REMPI spectrum of Fig 2 using an ionization energy of 6.7 eV, which is significantly *below* that of *ipso* according to our calculations. The ensuing spectrum does not reveal any missing peaks, compared with the spectrum in Fig 2. Therefore we have found no evidence of any spectral signature of the *ipso* isomer in the spectral range 480 – 617 nm.

We conclude that, in a molecular beam resulting from discharge of phenol/water/argon, the resulting H-atom reaction with phenol produces predominantly the *ortho*-hydroxy-CHD radical. There is no evidence for *para* or *ipso*, and there is tentative evidence for <1% *meta* isomer.

H and D-addition to toluene: methylcyclohexadienyl radical (methyl-CHD)

A similar set of experiments was performed for the reaction of H-atoms with toluene. Figure 5 shows the (1+1') REMPI spectrum of a molecule(s) with m/z 93, the mass of H + toluene. The PIE curve, measured when the first REMPI laser was tuned to the large peak near $18,300\text{ cm}^{-1}$, is shown at the top of Fig 3. After correction for the extraction field in the same way as previously, the IE of this molecule was determined to be $6.5862(5)\text{ eV}$.¹³

The same set of calculations, at the same level of theory, was performed on the four isomers of methyl-CHD (Table 4). At this level of theory, we empirically correct the IEs by -80 meV , in keeping with the benchmark study above, and also validated by the results on the hydroxy-CHD radical. The corrected IE of the *ipso* isomer clearly does not match the experimental value. The IEs of the *ortho*, *meta* and *para* isomers are clustered

more closely together than they were for hydroxy-CHD. Nonetheless, attribution of the m/z 93 carrier of the peak at 18290 cm^{-1} to the *ortho* isomer is the only one that lies within the computational uncertainty, which we estimate at $<100\text{ meV}$.⁵²

The REMPI spectrum in Fig 5 shows a complex set of close, but irregularly spaced peaks in the region assigned as the electronic origin. By analogy with the spectroscopy of the toluene⁵³⁻⁵⁸ and singly-substituted toluenes,⁵⁹⁻⁶¹ this structure is assigned as arising from methyl-rotor torsional vibrations. Methyl-rotor structure in toluene itself and in substituted toluenes, has been well studied. The methyl-rotor torsional states are of very low energy, and the spacing between levels depends sensitively on the height and form of the torsional barrier. In toluene, and toluene with other atoms substituted in the *para*-position, the potential is six-fold symmetric. Introduction of a substituent at the *ortho* or *meta* position introduces a three-fold term into the potential.

The energy levels of the internal rotation of the methyl rotor are usually represented by the quantum number of a free one-dimensional rotor, m , where $m = 0, \pm 1, \pm 2, \dots$. For a free rotor, the levels have energy proportional to m^2 . For a hindered rotor, the energy level spacings are irregular, with the energies a sensitive function of the shape of the torsional potential. For a potential with three-fold symmetry, such as *ortho*-methyl-CHD, the levels have symmetry designations of a and e . The $m = \pm 3n$ levels (where n is an integer) are of a symmetry, while $m = 3n \pm 1$ levels are e .

Electronic transitions between different methyl rotor states are subject to symmetry selection rules. For a potential with six-fold symmetry, the transitions are dominated by $\Delta m = 0$, although $\Delta m = 3$ are also observed. The recent papers by Lawrance provide an excellent description of methyl-rotors in the spectroscopy of toluene.⁵⁶⁻⁵⁶ For a potential of three-fold symmetry, the selection rules are $a \star a$ and $e \star e$.

The methyl-rotor vibrational structure in the electronic spectrum is also a sensitive function of the change in torsional potential upon electronic excitation. In toluene and *p*-fluorotoluene, there is little change in the equilibrium rotor position and the spectrum shows only weak activity in the methyl rotor modes. In *ortho*-substituted toluene, the V_3 term is much larger than in the *meta*-substituted counterparts, due to the increased steric interaction.⁵⁹ The change in V_3 can also be significant upon electronic excitation

*H-addition to phenol and toluene**submitted to PCCP*

for the *ortho*-species; in fluorotoluene, the minimum in S_0 becomes a maximum in S_1 .⁵⁹ For the *meta* equivalent, the minimum lies at the same angle in S_0 and S_1 , with the consequence that the torsional structure in *m*-fluorobenzene is also dominated by $\Delta m = 0$.⁵⁹ The extensive torsional structure in the spectrum in Fig 5 is therefore consistent with the formation of *ortho*-methyl-CHD, and not *meta* or *para*.

There are more peaks in the origin region than can be accounted for by a single methyl rotor progression and it is clear that other low frequency vibrations play an important part of the spectroscopy in this region. Other vibrations, however, can have a profound effect on the torsional potential.^{57,58} For example, the ring-breathing vibration, ν_1 , and in-plane ring-distortion, ν_6 , again form the dominant progressions in Fig 5. Each has a similar set of torsional transitions associated with them. The spacings between the peaks in the ν_1 progression are similar, but not exactly the same, as the origin region. For the ν_6 progression, however, they quite different, which is apparent by eye in Fig 5.

To untangle the spectrum, we have performed the same experiment using a combination of deuterated toluenes (toluene- d_3 , and $-d_8$) and normal and deuterated water (D_2O). This gives rise to 6 different isotopologues of *ortho*-methyl-CHD. The torsional energy levels shift significantly when the CH_3 -group is deuterated, as expected, but not so much when the CH_2 group is deuterated. This has allowed us to unpack the spectrum and separate low frequency skeletal vibrations from methyl torsion vibrations. The torsional structure for the origin is assigned in Fig 5, along with the torsional structure neighboring the ν_{6a} and ν_1 progressions. Another torsional progression is indicated threaded through the origin series, which has its origin in one of the low frequency out-of-plane skeletal vibrations.

The experiments on specifically deuterated toluene and water were also used to clarify another aspect of the H + toluene reaction, which is important in later discussion of the H-addition mechanism. The resultant m/z 94 (D + toluene) REMPI spectrum is almost identical to that for the fully hydrogenated radical, evincing a CH_3 rotor (i.e. no D-atom substitution on the rotor position). No evidence of other isotopomers (D-addition elsewhere on the ring or on the rotor) was found. In addition, no evidence for other isotopologues (greater substitution of D-atoms) was found in the mass spectrum.

Experiments were further repeated using toluene- d_3 (CD_3 rotor) and toluene- d_8 reacting with both H atoms and D atoms. In every case, we only observed single addition of H/D to the *ortho* site on the ring – no other isomers, and no additional substitution of H for D, or vice versa.

The above observations indicate clearly that the H-addition process for toluene (and presumably phenol) is a single-step kinetic pathway. The spectra show clearly that there is no intramolecular H/D exchange. The mass spectra show clearly that there are no sequential reactions involving H/D-addition, followed by H/D loss that would otherwise mix up the resultant isotopologues, resulting in new mass channels. These observations provide strong evidence that the observed radicals are the result of a single H or D-addition reaction. If the *ortho*-methyl-CHD($-d_1$) radical that is formed from the toluene + D reaction spontaneously lost H or D from the sp^3 site, then both toluene- d_0 and toluene- d_1 would be formed. Subsequent reaction of D atoms with toluene- d_1 would lead to two isomers of *ortho*-methyl-CHD($-d_2$), with either both D atoms on the same carbon, or with D substitution on both *ortho* positions. Sequential addition / loss reactions would lead to increasing deuteration of the radical at the *ortho* position, an effect that was not observed.

Again, we searched for evidence of the *para*, *meta* and *ipso* isomers by scanning up to 2000 cm^{-1} to higher and lower frequency than the *ortho* origin bands. Spectra were re-taken with different ionization energies and no features in the spectrum appeared or disappeared. Therefore, like hydroxy-CHD, we conclude that only the *ortho*-methyl-CHD radical is formed to a significant extent in these experiments.

A complete analysis of the spectrum in Fig 5 and spectra of the isotopologues of methyl-CHD, including fitting the torsional potential in both D_0 and D_1 states of all 6 isotopologues, is beyond the scope of the present work. This extensive spectroscopic work will be published in a forthcoming paper.

Discussion

The results above report the $D_1 \leftarrow D_0$ spectra of *ortho*-methyl-cyclohexadienyl radical and both *syn* and *anti* conformers of the *ortho*-hydroxy-CHD radical, which were formed

*H-addition to phenol and toluene**submitted to PCCP*

from H-addition to toluene and phenol, respectively. The spectra have sharp structure in each case, with well-resolved vibrational transitions, and a D_1 lifetime for hydroxy-CHD that has been measured in the 3-5 ns range. Adiabatic (0 K) ionization energies were measured for each isomer.

Ab initio and DFT calculations support the experimental results. Benchmarking to the CHD radical provided an empirical correction for the ionization energies calculated using G4(MP2)-6X theory. When this correction was applied to calculations on the *ortho*-methyl- and *ortho*-hydroxy-CHD radicals, the experimental IEs were reproduced to within 10 meV.

The most intriguing aspect of this work is that we have identified and assigned only the *ortho* isomer for H-atom addition to phenol and toluene. No evidence was found for the formation of the *ipso* or *para* isomers. Tentative evidence for a small amount of the *meta* isomer of hydroxy-CHD was presented, but no evidence of the *meta* isomer for the methyl-substituted radical. It is this aspect of the H-addition chemistry that we focus on in this discussion.

***Ab initio* calculations on H-addition to phenol and toluene**

Figure 6 shows the energies for stationary points on the reaction paths for H-addition to phenol and toluene, OH- or CH₃-addition to benzene, and [1,2]-H shifts between the various substituted cyclohexadienyl radical isomers. The calculations were performed at a single level of theory, *vis* G4(MP2)-6X//B3-LYP/6-31G(2df,p). In both cases, the *ortho* isomer is the most stable, lying 12-13 kJ mol⁻¹ below *meta* and *para* for the hydroxy-CHD radical, but only 5-7 kJ mol⁻¹ lower for methyl-CHD. The *ipso* isomer, which is the essential isomer connecting H + phenol (toluene) and OH (CH₃) + benzene, lies 32 and 11 kJ mol⁻¹ higher in the respective radicals. Not shown in the figure are the *syn* and *anti* conformers of the *meta* and *ortho* isomers.

The hydroxy-CHD potential energy surface: Some of these energies and pathways have been calculated previously for hydroxy-CHD,^{27,28,29} but, to our knowledge, none of the previous studies characterized all of the isomers and transition structures.

Consequently, there is not a complete picture of the chemistry from benzene + OH to phenol + H that includes all the isomers and transition states such as shown in Fig 6a).

The most studied part of this potential energy surface is the benzene + OH reaction because of its importance in atmospheric and combustion chemistry. This reaction leads solely to the *ipso* isomer, although other reaction products, including displacement of OH for H leading directly to phenol, have also been postulated to be competitive with OH-addition.^{26,30} Previous calculations of the stability of the *ipso* isomer lie in the range -66 to -78 kJ mol⁻¹ relative to phenol + H with an entrance channel barrier of 26 to 41 kJ mol⁻¹.^{27,28,29} The energies of the other isomers have been calculated by Sander *et al.*²⁷ Their hydroxy-CHD energies are slightly lower with respect to phenol + H than ours, but were not corrected for zpe. Our uncorrected energies (Table 2) are similar to the previous values.

Given the observation of only the *ortho* isomer, which is most stable, we were interested in whether (1,2)-H transfer between isomers might be possible. The TS energies for transfer from *ipso-ortho*, *ortho-meta* and *meta-para* were therefore calculated. The results displayed in Fig 6 show clearly that the TSs lie significantly (>100 kJ mol⁻¹) above the TS for breaking the C-H bond. The same phenomenon has been calculated for H-D scrambling in CHD radical itself – the energy of the TS for [1,2]-H shift in CHD was twice as high as that for removing the *sp*³ H-atom.^{32,62}

The potential energy surface for the methyl-CHD radical is quite similar to that of the OH analog (Fig 6b). [1,2]-H shifts in methyl-CHD have transition states that lie well above the TS for C-H cleavage, which is ~ 110 kJ mol⁻¹. The energy ordering of the isomers is the same: *ortho* < *meta* < *para* < *ipso*. But *ortho* is favoured by only 5-7 kJ mol⁻¹. The entrance channel barriers from toluene + H into the methyl-CHD wells are larger than for phenol + H, being ~ 30 kJ mol⁻¹ instead of ~ 20 kJ mol⁻¹. The *ortho* TS remains the lowest, with a difference between this and the *para* and *meta* TSs still ~ 5 kJ mol⁻¹.

Therefore we conclude that the observed preference for *ortho*-addition of H to toluene and phenol must lie in the formation process, rather than subsequent migration of the H-atom around the ring.

Is the detection method biased towards *ortho*?

Our characterization technique is (1+1') resonance-enhanced multiphoton ionization coupled with time-of-flight mass spectrometry. The energy of D_1 is clearly well above the C-H bond dissociation energy and hence the transition is pre-dissociative. Therefore we must consider the possibility that the *ortho* isomer is longer-lived in the D_1 state than the other isomers. The measured lifetime of the *ortho* isomer is 3-5 ns. However, we have been successful in detecting radicals with excited state lifetimes as short as ~100 ps, inferred from their spectral linewidth. Therefore the lifetime of the other hydroxy- or methyl-CHD isomers would therefore need to be >50× shorter than that of the observed *ortho* isomers for REMPI to be an ineffective technique. Given the very similar electronic properties of the four isomers, we have no reason to suspect that this is so.

We also note a much older work by Bennett and Mile in 1973.⁶³ In this remarkable, but little cited work, they measured the products of H and D addition to ~30 unsaturated and aromatic compounds by bombardment of a cold matrix of olefin by H/D atoms. They observed that for toluene [ϕ -CH₃], benzyl alcohol [ϕ -CH₂OH] and cumene [ϕ -CH(CH₃)₂], the H/D addition occurs solely at the *ortho* position. In contrast to our work, they observed a much smaller amount of *para* isomer, and no evidence of *meta*. The notable feature for the present discussion is that their detection technique was ESR spectroscopy, which has no bias towards *ortho*, *meta* or *para* and no reliance on excited state spectroscopy. Therefore we conclude that the addition of H to toluene and phenol is *ortho*-directed.

Energetic considerations

The *ortho* isomer is the lowest lying of the isomers, for both hydroxy- and methyl-CHD. It lies 12-13 kJ mol⁻¹ below *meta* and *para* for the OH structure, but only 5-7 kJ mol⁻¹ lower for the CH₃ structure. Our first consideration, therefore, is whether energetic considerations alone can account for the *ortho* preference.

Generally, a supersonic expansion of discharge products is not a discriminating technique. Many radicals are formed – not solely the thermodynamically-favoured product. For example, in the same instrument we observed the *cis* and *trans*-

vinylpropargyl molecule (C_5H_5),⁶⁴ even though it lies 130 kJ mol^{-1} above the global minimum, the *c*-pentadienyl radical.⁶⁵ Even in the present work, both *syn* and *anti* conformers of *ortho*-hydroxy-CHD are observed strongly even though *syn* lies 6 kJ mol^{-1} above the *anti*. This is similar to the energy difference between *ortho* and *para/meta*-methyl-CHD ($5\text{-}7 \text{ kJ mol}^{-1}$), yet only *ortho* is observed. Therefore it seems unlikely that the preference for the *ortho*-isomers is driven by thermodynamics alone.

Kinetic considerations

The height of the barrier in the entrance channel determines the kinetic preference for various isomers. For both substituted-CHD radicals, the *ortho* isomer has the lowest energy entrance channel barrier of the four structural isomers. For OH, this is 20 kJ mol^{-1} , compared with 24 kJ mol^{-1} for both *meta* and *para*, and 37 kJ mol^{-1} for the *ipso* isomer. For CH_3 , the entrance barriers are: 24 kJ mol^{-1} for *ortho*, 29 kJ mol^{-1} for *para* and *meta* and 32 kJ mol^{-1} for *ipso*.

The collision conditions in a discharge expansion are difficult to characterize. Collisions within the region of the electrodes can be very energetic, but collisions late in the supersonic expansion are considerably colder than room temperature. If we assume that the entrance channels are similar in topology (entropy), then, working in reverse, we can calculate the effective temperature required to achieve an order of magnitude difference in formation rate, given the barriers in Fig 6. For a difference in barrier height of 4 kJ mol^{-1} in the entrance channel (hydroxy-CHD), a collision temperature of 200 K would produce a ten-fold enhancement in reaction rate for the compound with the lower barrier compared with the higher barrier channel, irrespective of the barrier height (exclusive of symmetry effects, which enhances *ortho* and *meta* over *para* and *ipso* by a further factor of two by virtue of the number of identical sites). At 100 K , the difference would be 100-fold. Indeed, a translational temperature of $100\text{-}200 \text{ K}$ is what would be expected in the early stages of a supersonic expansion.

At this stage, it is appropriate to consider the experiments on deuterium addition to toluene. As discussed above, when D_2O was used instead of H_2O , the only product was methyl-CHD- d_1 . If the reaction proceeded at high translational temperature, one would expect that some of the transiently formed methyl-CHD radicals would spontaneously

*H-addition to phenol and toluene**submitted to PCCP*

decompose back to toluene + H/D. Consideration of zero-point energy for H-loss and D-loss would favour the H-loss channel, so we would expect methyl-CHD- d_1 to produce a significant amount of toluene- d_1 + H, which would then further react with D atoms to form methyl-CHD- d_2 . We observed no evidence of the $-d_2$ isotopologue in the mass spectrum. Therefore we conclude that there is no further processing of toluene via reaction with D-atoms. This is best explained by requiring the energy of the first D + toluene reaction to be fairly low, so that a single collision with the cold Ar carrier gas stabilizes the methyl-CHD radical. This is consistent with a collision temperature of 100-200 K.

Finally, it is pertinent to consider the effect of tunneling of H-atoms in both the formation and decomposition of substituted CHD radicals. The principal effect of tunneling is to lower the effective barrier for both H-addition and H-loss channels. If the effects of tunneling are similar for all isomers, then this has no effect on the discussion above; the preference for one channel over another depends on the difference in barrier height, not the barrier height itself. Lowering the barrier of both channels by the same amount will increase the rate of reaction (increasing the signal in the experiment), but it will not change the relative yield of one channel over another.

We therefore conclude that our data are consistent with a preference for *ortho*-addition to phenol and toluene caused by a kinetic effect at a temperature of 100-200 K.

Implications for combustion modeling

Rate constants for the reactions of H-atoms with benzene, phenol and toluene have all been measured for a wide range of temperatures relevant to combustion.⁶⁶ The competition between H-abstraction and H-addition is a sensitive function of temperature. As a general rule, the importance of abstraction over addition increases with temperature. For example, at $T < 600$ K, the rate constant for H-addition to toluene to form methyl-CHD, is larger than H-abstraction to form H₂ + benzyl radical, or benzene + CH₃. For $T > 600$ K, both abstraction reactions have rate constants that are larger than the H-addition.⁶⁶ Similarly, for H + benzene, H-addition is the only important mechanism for all except the most elevated combustion temperatures.⁶⁶

Despite the importance of H-addition to aromatic species in combustion, there are no studies in which the isomer-specific products of such addition have been elucidated. In this work, we determined that H-addition to phenol and toluene, at a temperature of 100-200 K is significantly (>10-fold) *ortho*-directed. When taken in concert with the results of Bennett and Mile,⁶³ it is strongly suggestive that preferential *ortho*-addition is the norm for many singly-substituted benzenes.

Using the energetics (barriers) and relative kinetics employed above, we can predict the *ortho*-directing effect at increased temperatures more relevant to combustion. Using the calculated barriers for toluene in Fig 6b, we predict that at 600 K, *ortho*-methyl-CHD would be kinetically-preferred over *meta* by a factor of ~3, and over *para* by ~6, due to symmetry considerations. *Ips*o remains less favored by more than a factor of 10 for methyl-CHD at this temperature.

At 2000 K, the predicted relative rates still favor the formation of the *ortho* product, with a ratio of *ortho* : *meta* : *para* : *ip*so of 1 : 0.7 : 0.35 : 0.3. At even more elevated temperatures, the relative rates of formation of *ortho*, *meta*, *para* and *ip*so converge on the symmetry-imposed ratio of 1 : 1 : 0.5 : 0.5.

Conclusions

We have studied the formation of hydroxy- and methyl-cyclohexadienyl radicals via the reaction of H and D atoms with phenol and toluene, respectively. The 1+1' REMPI spectrum and the adiabatic ionization energies of these species are reported. The experiments were accompanied by extensive quantum chemical calculations, which were benchmarked to the well-known cyclohexadienyl radical. We report calculated energies and structures for *ortho*, *meta*, *para* and *ip*so isomers of the two substituted-CHD radicals, including *syn* and *anti* conformers of *ortho* and *meta* isomers. Transition structures for H migration around the ring are reported, as are the transition structures for both H + toluene/phenol and OH/CH₃ + benzene.

In all cases, the REMPI spectra can be assigned solely to H-atom attachment at the *ortho* position. There is no experimental evidence for any other isomer, except for a hint of *meta*-hydroxy-CHD in the H + phenol experiments. For the case of D-addition, no further

deuteration other than a single D-atom was observed, attesting to H/D addition being a primary reaction with no recycling of H and D atoms via the reverse reaction.

We attribute the greater than tenfold preference for formation of *ortho* radicals to the height of the barrier in the entrance channel to the reaction, which is 4-5 kJ mol⁻¹ lower for *ortho* than *meta* and *para* and even further below the *ipso* channel. Under the conditions of these experiments, this is consistent with formation of the radicals at a collision temperature of 100-200 K, appropriate for the early stages of a molecular beam expansion. Under pre-ignition conditions in combustion (T = 200 – 400°C), we predict *ortho* to be still the significantly preferred product. Only at an elevated temperature (T > 2000°C) would the formation rate of the three lower-energy isomers approach the statistical ratio of 1 : 1 : 0.5 : 0.5 for *ortho* : *meta* : *para* : *ipso*.

Acknowledgements

This work was supported by the Australian Research Council (grant DP120102559). CMW acknowledges an Australian Postgraduate Award scholarship. We gratefully acknowledge generous allocations of supercomputer time from the National Computational Infrastructure (NCI) National Facility and Intersect Australia Ltd.

REFERENCES

- (1) For example, C. K. Westbrook, *Combustion and Flame*, 2009, 156, 181.
- (2) For example, B. J. Finlayson-Pitts, J. N. Pitts, Jr., *Chemistry of the Upper and Lower Atmosphere*, (Academic Press, 2000).
- (3) D. U. Andrews, B. R. Heazlewood, A. T. Maccarone, T. Conroy, R. J. Payne, M. J. T. Jordan, S. H. Kable, *Science*, 337, 1203
- (4) For example, J. A. Rasmussen, *J. Phys. Chem. A* 2013, 117, 4279.
- (5) E. Habart, F. Boulanger, L. Verstraete, G. Pineau des Forets, E. Falgarone, A. Abergel, *Astron. Astrophys.* 2003, 397, 623.
- (6) D.L. Kokkin and T.W. Schmidt, *J. Phys. Chem. A*, 2006, 110, 6173.

-
- (7) "Fuel Standard (Petrol) Determination 2001", Office of Legislative Drafting and Publishing, Commonwealth of Australia
- (8) A. Tesner, *Proc. Combust. Inst.* 1958, 7, 546.
- (9) T. Bera, J. W. Thybaut, G. B. Marin, *Ind. Eng. Chem. Res.* 2011, 50, 12933.
- (10) T. Shida, I. Hanazaki, *Bull. Chem. Soc. Japan*, 1970, 43, 646.
- (11) T. Imamura, W. Zhang, H. Horiuchi, H. Hiratsuka, T. Kudo, and K. Obi, *J. Chem. Phys.*, 2004, 121, 6861.
- (12) M. Nakajima, T. W. Schmidt, Y. Sumiyoshi, Y. Endo, *Chem. Phys. Lett.*, 2007, 449, 57.
- (13) O. Krechkivska, C. Wilcox, G. D. O'Connor, K. Nauta, S. H. Kable, T. W. Schmidt, *J. Phys. Chem. A*, 2014, 118, 10252.
- (14) A. Bonaca, G. Bilalbegovic, *Mon. Not. R. Astron. Soc.* 2011, 416, 1509–1513.
- (15) J. A. Sebree, V. V. Kislov, A. M. Mebel, T. S. Zwier, *J. Phys. Chem. A*, 2010, 114, 6255–6262.
- (16) M. Bahou, Y.-J. Wu, Y.-P. Lee, *Phys. Chem. Chem. Phys.* 2013, 15, 1907–1917
- (17) O. Krechkivska, Y. Liu, K. L. K. Lee, K. Nauta, S. H. Kable, T. W. Schmidt, *J. Phys. Chem. Lett.* 2013, 4, 3728.
- (18) O. Krechkivska, C. M. Wilcox, B. Chan, R. Jacob, Y. Liu, K. Nauta, S. H. Kable, L. Radom, T. W. Schmidt, *J. Phys. Chem. A*, 2015, 119, 3225.
- (19) J. G. Calvert, R. Atkinson, K. H. Becker, R. M. Kamens, J. H. Seinfeld, T. J. Wallington, G. Yarwood, "The Mechanisms of Atmospheric Oxidation of Aromatic Hydrocarbons" (Oxford University Press: New York, 2002).
- (20) A. Bargholz, R. Oswald and P. Botschwina, *J. Chem. Phys.* 2013, 138, 014307.
- (21) W. H. Hamill, J. P. Guarino, M. R. Ronayne and J. A. Ward, *Disc. Faraday Soc.*, 1963, 36, 169.
- (22) J. E. Jordan, D. W. Pratt, D. E. Wood, *J. Am. Chem. Soc.* 1974, 96, 5588.
- (23) I. Garkusha, J. Fulara, A. Nagy, J. P. Maier, *J. Am. Chem. Soc.* 2010, 132, 14979.
- (24) C.-C. Chen, J. W. Bozzelli, J. T. Farrell, *J. Phys. Chem. A*, 2004, 108, 4632.
- (25) R. Volkamer, B. Klotz, I. Barnes, T. Imamura, K. Wirtz, N. Washida, K. H. Becker, U. Platt, *Phys. Chem. Chem. Phys.* 2002, 4, 1598
- (26) B. Fritz, V. Handwerk, M. Preidel, R. Zellner, *Ber. Bunsenges. Phys. Chem.* 1985, 89, 343.

-
- (27) A. Mardyukov, R. Crespo-Otero, E. Sanchez-Garcia, W. Sander, *Chem. Eur. J.* 2010, 16, 8679.
- (28) C.-C. Chen, J. W. Bozzelli, J. T. Farrell, *J. Phys. Chem. A.* 2004, 108, 4632.
- (29) I. V. Tokmakov, M. C. Lin, *J. Chem. Phys.* 2002, 116, 11309.
- (30) E. Bjergbakke, A. Sillesen, P. Pagsberg, *J. Phys. Chem.* 1996, 100, 5729.
- (31) V. H. Uc, A. Hernandez-Laguna, A. Grand, A. Vivier-Bunge, *Phys. Chem. Chem. Phys.*, 2002, 4, 5730.
- (32) I. V. Tokmakov, M. C. Lin, *Int. J. Chem. Kin.* 2001, 33, 633.
- (33) N. J. Reilly, M. Nakajima, T. P. Troy, N. Chalyavi, K. A. Duncan, K. Nauta, S. H. Kable, T. W. Schmidt, *J. Am. Chem. Soc.* 2009, 131, 13423.
- (34) H. Snyder, B. Smith, T. Parr, R. Martin, *Chem. Phys.* 1982, 65, 397.
- (35) M. J. Frisch, G. W. Trucks, H. B. Schlegel, G. E. Scuseria, M. A. Robb, J. R. Cheeseman, G. Scalmani, V. Barone, B. Mennucci, G. A. Petersson, *et al.*, Gaussian 09, Revision A.02; Gaussian, Inc.: Wallingford, CT, 2009.
- (36) H-J. Werner, P. J. Knowles, G. Knizia, F. R. Manby, M. Schütz, P. Celani, T. Korona, R. Lindh, A. Mitrushenkov, G. Rauhut, *et al.*, *MOLPRO*, 2010.1; University College Cardiff Consultants Limited: Cardiff, UK, 2010.
- (37) D. J. Henry, M. J. Sullivan, L. Radom, *J. Chem. Phys.* 2003, 118, 4849–4860.
- (38) B. Chan, J. Deng, L. Radom, *J. Chem. Theory Comput.* 2011, 7, 112–120.
- (39) B. Chan, L. Radom, *J. Chem. Theory Comput.* 2012, 8, 4259–4269.
- (40) A. D. Boese, J. M. L. Martin, *J. Chem. Phys.* 2004, 121, 3405–3416.
- (41) J. P. Merrick, D. Moran, L. Radom, *J. Phys. Chem. A*, 2007, 111, 11683–11700.
- (42) A. J. Birch, A. L. Hinde and L. Radom, *J. Am. Chem. Soc.* 1980, 102, 4075
- (43) F. Berho, M.-T. Rayez and R. Lesclaux, *J. Phys. Chem. A*, 1999, 103, 5501.
- (44) *NIST Chemistry WebBook, NIST Standard Reference Database Number 69*, Eds. P.J. Linstrom and W.G. Mallard, National Institute of Standards and Technology, Gaithersburg MD, 20899
- (45) D. Aue, M. Guidoni, L. Betowski, L. *Int. J. Mass Spectrom.* 2000, 201, 283.
- (46) E. P. L. Hunter, S. G. Lias, *J. Phys. Chem. Ref. Data*, 1998, 27, 413
- (47) E. B. Wilson, Jr, *Phys. Rev.*, 1934, 45, 706.
- (48) P. Butler, D. B. Moss, H. Yin, T. W. Schmidt, S. H. Kable, *J. Chem. Phys.* 2007, 127, 094303.

-
- (49) A. K. Swinn, S. H. Kable, *J. Molec. Spectrosc.*, 1998, 191, 49.
- (50) G. H. Atkinson, C. S. Parmenter, *J. Molec. Spectrosc.*, 1978, 73, 52.
- (51) A. G. Gardner, T. G. Wright, *J. Chem. Phys.*, 2011, 135, 114305.
- (52) T.P. Troy, N. Chalyavi, A. S. Menon, G. D. O'Connor, B. Fückel, K. Nauta, L. Radom, T. W. Schmidt, *Chem. Sci.* 2011, 2, 1755.
- (53) P. J. Breen, J. A. Warren, E. R. Bernstein, J. I. Seeman, *J. Chem. Phys.* 1987, 87, 1917.
- (54) D. B. Moss, C. S. Parmenter, and G. E. Ewing *J. Chem. Phys.* 1987, 86, 51
- (55) A. M. Gardner, A. M. Green, V. M. Tamé-Reyes, V. H. K. Wilton, T. G. Wright, *J. Chem. Phys.* 2013, 138, 134303.
- (56) J. R. Gascooke, W. D. Lawrance, *J. Chem. Phys.* 2013, 138, 134302.
- (57) J. R. Gascooke, E. A. Virgo, W. D. Lawrance, *J. Chem. Phys.* 2015 142, 024315.
- (58) J. R. Gascooke, E. A. Virgo, W. D. Lawrance, *J. Chem. Phys.* 2015, 143, 044313.
- (59) K. Okuyama, N. Mikami, M. Ito, *J. Phys. Chem.* 1985, 89, 5617.
- (60) Z-Q. Zhao, C. S. Parmenter, D. B. Moss, A. J. Bradley, A. E. W. Knight, K. G. Owens, *J. Chem. Phys.* 1992, 96, 6362.
- (61) T-Y. D. Lin, T. A. Miller, *J. Phys. Chem.* 1990, 94, 3554.
- (62) O. Kikuchi, S. Shimomura, *Bull. Chem. Soc. Japan*, 1984, 57, 2993
- (63) J. E. Bennett, B. Mile, *J. Chem. Soc, Faraday Trans.* 1973, 69, 1398.
- (64) N. J. Reilly, M. Nakajima, T. P. Troy, N. Chalyavi, K. A. Duncan, K. Nauta, S. H. Kable, T. W. Schmidt, *J. Am. Chem. Soc.* 2009, 131, 13423
- (65) L. V. Moskaleva, M. C. Lin, *J. Comput. Chem.* 1999, 21, 415.
- (66) D. L. Baulch, *et al.*, *J. Phys. Chem. Ref. Data*, 2005, 34, 757

Tables:**Table 1:** Experimental and theoretical results on the cyclohexadienyl radical. All units are kJ mol^{-1} , except for the ionization energy, which is reported in eV.

Level of theory	Ionization Energy (eV)	C_6H_6 Proton Affinity	$\text{C}_6\text{H}_7 \rightarrow \text{C}_6\text{H}_6 + \text{H}$	$\text{C}_6\text{H}_7^+ \rightarrow \text{C}_6\text{H}_6^+ + \text{H}$
B3-LYP / 6-31G(2df,p)	6.45	810	119	352
B3-LYP / 6-311++G(3df,3pd)	6.69	788	114	351
G3X(MP2)-RAD	6.86	765	110	355
G4(MP2)-6X vibrationless	6.85	766	107	353
G4(MP2)-6X (zpe corrected, 0 K)	6.90	740	85	322
G4(MP2)-6X (zpe corrected, 298 K)	6.90	744	90	328
W1X-1 vibrationless	6.79	768	110	356
W1X-1 (zpe corrected, 0 K)	6.84	742	88	323
W1X-1 (zpe corrected, 298 K)	6.84	746	93	330
(R)CCSD(T*) vibrationless (a)	6.75	-	107	-
(R)CCSD(T*) (zpe corr., 0 K) (a)	6.803(5)	-	85.7	-
(R)CCSD(T*) (zpe-corr., 298 K) (a)	-	-	89.2	-
Experiment	6.8201 (b)	748.4 (c)	-	328.2 (d)

a) Reference 20.

b) 0 K, Reference 13.

c) 298 K. This is the average of two recommended values by NIST, (ref 44) from original references 45 and 46.

d) 298 K. This value was determined from the thermodynamic cycle involving experimental IE of H-atom and benzene (ref 44) and the experimental proton affinity of benzene in the table.

Table 2: Computational results for various thermochemical properties of the four isomers of hydroxycyclohexadienyl radical. Results are presented for the G4(MP2)-6X level of theory; results for other levels of theory are reported in Supplementary Information. All values in kJ mol⁻¹, except for the IE, in eV.

Property of hydroxy-CHD	<i>ortho</i>	<i>meta</i>	<i>para</i>	<i>ipso</i>
Relative energy	0.0	13.5	13.1	32.0
Relative energy of cation	14.4	73.3	0.0	123.7
C-H bond dissociation energy, vibrationless	119	106	106	87
C-H BDE, zpe corrected, 0K	97	85	85	66
Ionization energy, vibrationless (eV)	6.39	6.86	6.11	7.19
Ionization energy, zpe corrected, 0 K (eV)	6.47	6.94	6.19	7.27
Ionization energy, empirically corrected, 0 K (eV)	6.39	6.86	6.11	7.19
Ionization energy, corrected experimental (eV)	6.3989 and 6.4091 (\pm 0.0010)			

Geometries optimized at B3-LYP/6-31G(2df,p).

Table 3: Computational results for various spectroscopic properties for cyclohexadienyl (CD) and several isomers of hydroxy-CHD radical. Results are presented for TD-DFT B3LYP/cc-pvtz level of theory. For the *ortho* and *meta* isomers there are two rotamers corresponding to the orientation of the OH bond in *syn* and *anti* configurations.

Isomer of	Vertical ^{a)}	T_{00} ^{b)}	T_{00} (exp)	Calc-exp	$f^c)$
hydroxy-CHD	cm ⁻¹				($\times 10^3$)
<i>syn-ortho</i>	22097	20095	18218 ^{e)}	1877	0.6
<i>anti-ortho</i>	22327	19956	18200 ^{e)}	1756	1.1
<i>syn-meta</i>	21527	19867	(17865) ^{f)}	2003	9.6
<i>anti-meta</i>	20971	19531	(17714) ^{f)}	1817	12
<i>para</i>	19597	17225	-	-	14.5
<i>ipso</i>	22426	- ^{d)}	-	-	1.8
CHD	22569	20437	18207 ^{g)}	2230	0.8

a) Vertical transition energy from the D_0 minimum.

b) Transition energy from $D_0(v''=0)$ to $D_1(v'=0)$.

c) Oscillator strength.

d) The *ipso* calculation at this level of theory would not converge (see text).

e) This work.

f) This work. Tentative.

g) Reference 12.

Table 4: Computational results for various properties of the four isomers of methylcyclohexadienyl radical (methyl-CHD). Results are presented for the G4(MP2)-6X level of theory; results for other levels of theory are reported in Supplementary Information. All values in kJ mol^{-1} , except for the IE, in eV.

Property	<i>ortho</i>	<i>meta</i>	<i>para</i>	<i>ipso</i>
Relative energy of methyl-CHD	0.0	5.4	6.5	10.5
Relative energy of methyl-CHD cation	5.9	19.7	0.0	33.7
C-H bond dissociation energy, vibrationless	115	110	109	105
C-H BDE, zpe corrected, 0K	93	88	87	81
Ionization energy, vibrationless (eV)	6.63	6.72	6.50	6.81
Ionization energy, zpe corrected, 0 K (eV)	6.67	6.76	6.54	6.85
Ionization energy, empirically corrected, 0 K (eV)	6.59	6.68	6.46	6.77
Ionization energy, corrected experimental (eV)	6.5862 ± 0.0005			

Geometries optimized at B3-LYP/6-31G(2df,p).

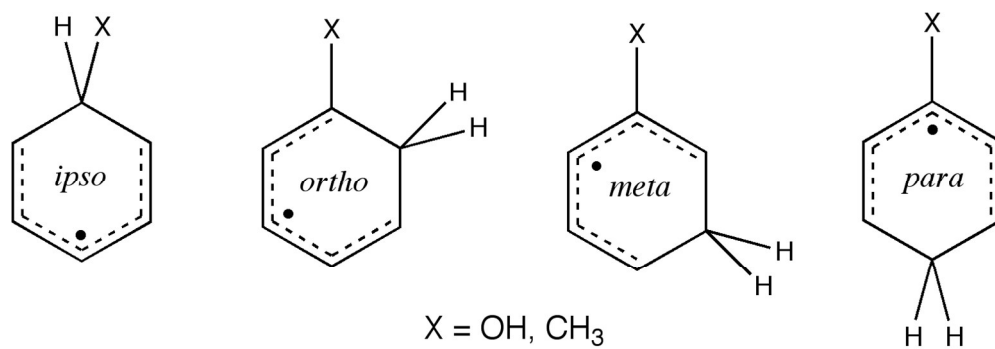


Figure 1: Four structural isomers of a singly-substituted cyclohexadienyl radical.
133x46mm (300 x 300 DPI)

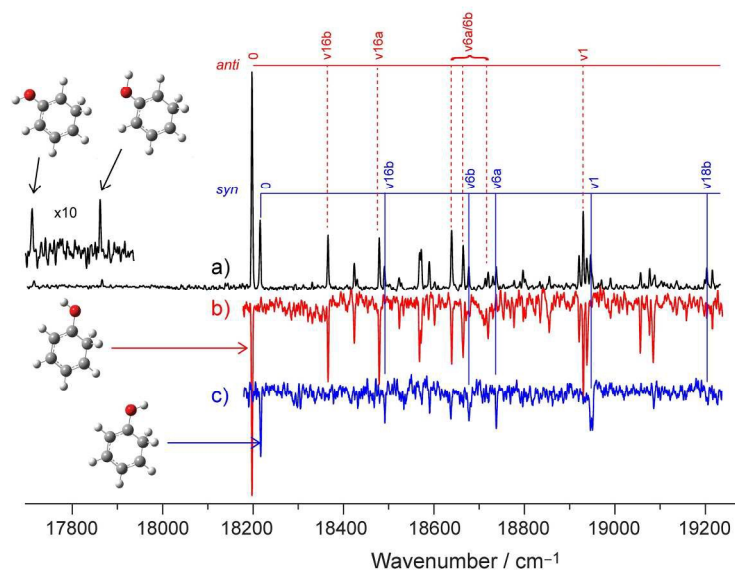


Figure 2: a) REMPI spectrum of m/z 95 species from H-addition to phenol. The carrier of the spectrum is assigned to be the syn and anti conformers of the ortho-hydroxycyclohexadienyl radical, as shown by comparison with the hole-burning spectra b) and c). Vibrational assignments of the most intense structure are shown above the REMPI spectrum, based on ab initio calculations of the D1 state of each conformer. Small features to the red of the main spectrum are tentatively assigned to the meta-hydroxy-CHD radical (see text).

209x148mm (300 x 300 DPI)

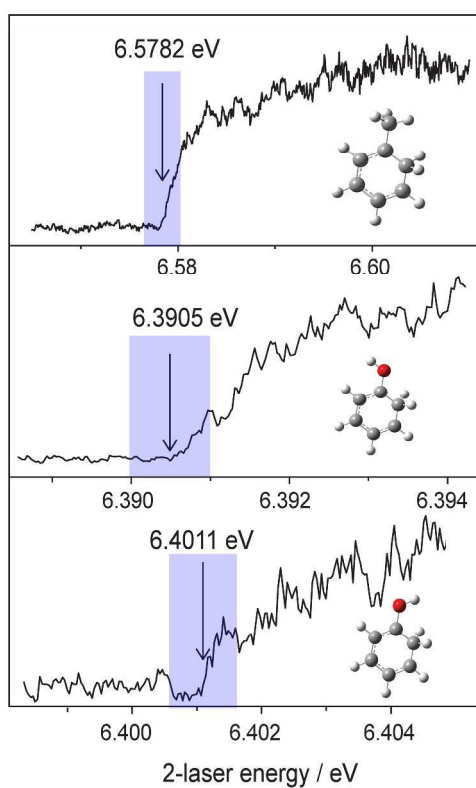


Figure 3: Photoionization efficiency curves for the three molecules studied in this work. The ionization energies indicated in the figure are for the molecules in a 206 V electric field, which lowers the IE by 8 meV. Corrected IEs are reported in Tables 1 – 3. Shaded regions represent an experimental uncertainty of 0.5 meV for methyl-CHD and 1 meV for hydroxy-CHD
297x420mm (300 x 300 DPI)

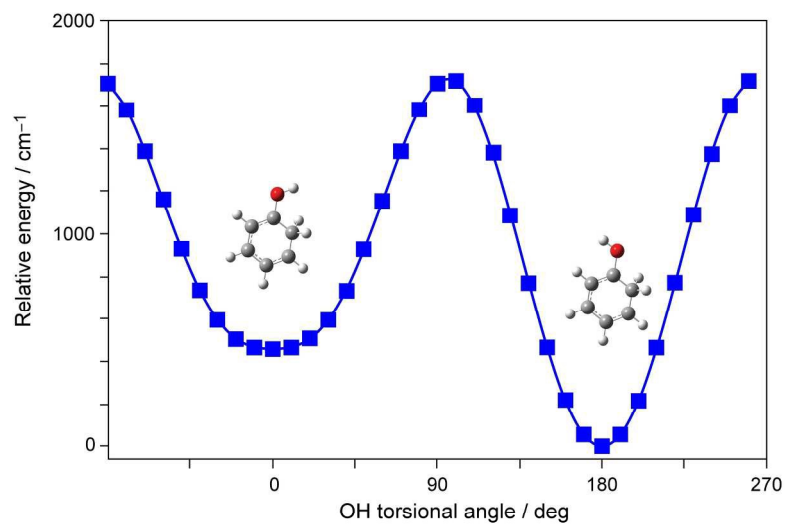


Figure 4: Potential energy scan of the OH torsional angle in ortho-hydroxy-CHD, computed at the B3-LYP/6-311++G(d,p) level of theory.
209x148mm (300 x 300 DPI)

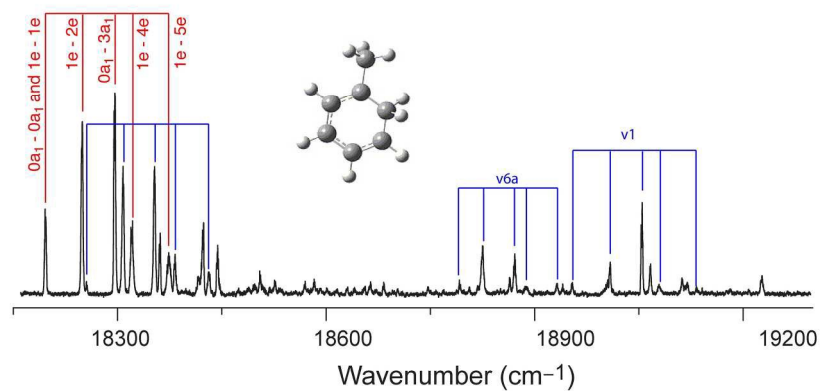


Figure 5: REMPI spectrum of the m/z 93 species formed from H-addition to toluene. The carrier of the spectrum is assigned to be ortho-methyl-cyclohexadienyl radical. The origin torsional progression is assigned, and three other torsional progressions are identified (see text).
209x148mm (300 x 300 DPI)

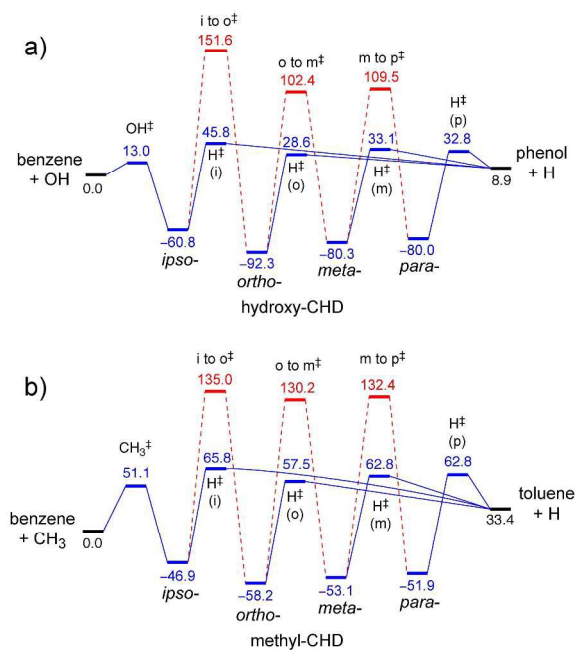


Figure 6: Energies (kJ mol⁻¹, 298 K) for stationary points on the reaction paths for a) H-addition to phenol through OH-addition to benzene and 1,2 H-transfer between the isomers of hydroxy-cyclohexadienyl radical; b) H-addition to toluene through CH₃-addition to benzene and 1-2 H-transfer between isomers of methyl-cyclohexadienyl radical. [[‡] represents a transition structure.] Values are calculated at G4(MP2)-6X//B3-LYP/6-31G(2df,p).
297x420mm (300 x 300 DPI)